American Mineralogist, Volume 85, pages 801–805, 2000

A new uranyl phosphate chain in the structure of parsonite

PETER C. BURNS

Department of Civil Engineering and Geological Sciences, University of Notre Dame, Notre Dame, Indiana 46556-0767, U.S.A.

ABSTRACT

The structure of parsonite, $Pb_2[(UO_2)(PO_4)_2]$, $Z = 2$, triclinic, space group $P\bar{1}$, $a = 6.842(4)$, $b = 10.383(6)$, $c = 6.670(4)$ Å, $\alpha = 101.26(7)°$, $\beta = 98.17(7)°$, $\gamma = 86.38(7)°$, $V = 459.8(7)$ Å^3, has been solved by direct methods and refined to $R = 6.0$ and a goodness-of-fit (S) of 0.92 using 1187 unique observed reflections ($|F| \geq 4\sigma_F$) collected with Mo$K\alpha$ X-rays and a CCD-based detector. The single unique U^{6+} cation is present as a $(UO_2)^{2+}$ uranyl ion (Ur) and is coordinated by five additional atoms of O arranged at the equatorial corners of a pentagonal bipyramid capped by the O_{Ur} atoms. Uranyl polyhedra share an edge-forming dimers, which are cross-linked by edge- and vertex-sharing with two distinct phosphate tetrahedra, resulting in a new uranyl phosphate chain. Two symmetrically distinct Pb^{2+} cations are coordinated by nine and six oxygen atoms, and link adjacent uranyl phosphate chains. Parsonite is the first uranyl phosphate mineral structure that is based upon chains of polymerized polyhedra of higher bond-valence; others contain sheets that are either based upon the autunite or phosphuranylite anion-topologies.

INTRODUCTION

The structural complexity of uranyl minerals challenges our understanding of low-temperature mineralogy. Considering the importance of uranyl minerals (e.g., Forsyth and Werme 1992; Finch and Ewing 1992; Johnson and Werme 1994; Pearcy et al. 1994; Finn et al. 1996; Wronkiewicz et al. 1996; Sowder et al. 1996; Murakami et al. 1997; Burns et al. 1997a, 1997b; Finch et al. 1998; Burns 1999; Burns and Finch 1999), it is regrettable that the structures remain unknown for ~2/3 of the 173 species. Experimental investigations of uranyl minerals are plagued by pseudosymmetry, small crystals, severe absorption of X-rays, complex intergrowths, large unit cells, and twinning. Theoretical approaches to modeling bonding have provided insight into mineral groups such as silicates, borates, and carbonates but remain intractable for all but the simplest of many-electron calculations involving U. The basis for understanding uranyl minerals must be experimentally determined crystal structures and relationships between mineral stabilities, paragenesis, and structures. Fortunately, the recent introduction of CCD-based X-ray detectors to mineralogy and synchrotron radiation for the analysis of micro crystals (Smith 1995) promise to significantly advance our knowledge of low-temperature minerals, especially groups such as uranyl minerals that have been intractable to conventional techniques.

Uranyl phosphates are significant for understanding the mobility of U in natural systems, and have received considerable attention (e.g., Murakami et al. 1997; Sowder et al. 1996). There are 45 uranyl phosphate minerals, but the structures are only known for fifteen. The structures of each are based upon sheets of vertex- and edge-sharing uranyl polyhedra and phosphate tetrahedra, and are grouped according to the details of the topological arrangement of the anions within the sheets (Burns et al. 1996). The autunite and phosphuranylite anion-topologies (Figs. 1a and 1c) are dominant in uranyl phosphates. Sheets based upon the autunite anion-topology (Fig. 1a) involve vertex-sharing between uranyl square bipyramids and phosphate tetrahedra (Fig. 1b). Sheets based upon the phosphuranylite anion-topology (Fig. 1c) contain uranyl pentagonal and hexagonal bipyramids that share edges to form chains, which are in turn cross-linked by sharing vertices and edges with phosphate tetrahedra (Fig. 1d).

Parsonite occurs at several localites, but only as micro crystals. Vochten et al. (1991) synthesized it by reacting synthetic chernikovite with a solution containing Pb. The currently accepted formula is $Pb_2(UO_2)(PO_4)_2(H_2O)_2$ (Mandarino 1999), which is unusual in the uranyl to phosphate ratio, and is inconsistent with a structure containing sheets based on the phosphuranylite or autunite anion-topologies. A specimen of parsonite with crystals that approach 100 μm in length was obtained, and data collected using a CCD-based diffractometer (Burns 1998) permitted the full determination of the structure, revealing a new uranyl phosphate structure-type.

EXPERIMENTAL METHODS

X-ray data

The specimen studied is from La Faye, Grury, Saone-le-Loire, France and contained mats of minute tabular crystals of parsonite. The largest crystal, with approximate dimensions $80 \times 30 \times 5$ μm^3, exhibited uniform optical properties and sharp extinction between crossed polarizers. It was mounted on a

*E-mail: pburns@nd.edu

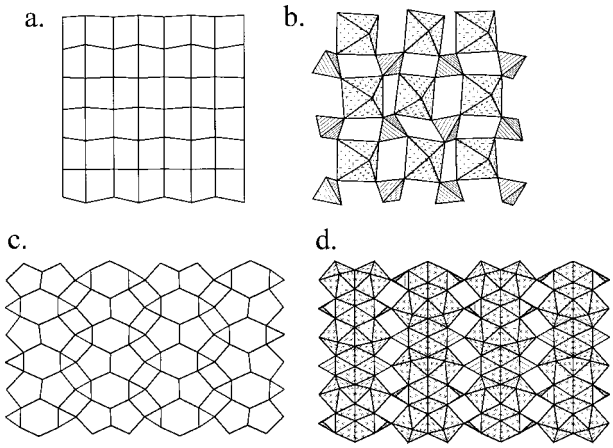

FIGURE 1. Uranyl phosphate sheets that are common in minerals. (**a**) autunite anion-topology, (**b**) autunite-type sheet, (**c**) phosphuranylite anion-topology, (**d**) phosphuranylite-type sheet. The uranyl polyhedra and phosphate tetrahedra are shaded with crosses and parallel lines, respectively.

Bruker Platform 3-circle goniometer equipped with a 1K SMART CCD (charge-coupled device) detector.

The data were collected using monochromatic Mo*K*α X-radiation and frame widths of 0.6° in ω, with 120 s used to acquire each frame. The long count time was essential to obtain reasonable counting statistics owing to the small size of the crystal. Unit-cell dimensions (Table 1) were refined on the basis of 1824 reflections using least-squares techniques. A sphere of three-dimensional data was collected for $3° \le 2\theta \le 56.7°$ in approximately 46 hours; comparison of the intensities of equivalent reflections collected at different times during the data collection showed no evidence of significant decay. The three-dimensional data were integrated and corrected for Lorentz, polarization, and background effects using the Bruker program SAINT. An empirical absorption-correction was done on the basis of the intensities of equivalent reflections using the program SADABS (G. Sheldrick, unpublished). Details are given in Table 1.

Structure solution and refinement

Scattering curves for neutral atoms, together with anomalous dispersion corrections, were taken from *International Tables for X-Ray Crystallography* (Ibers and Hamilton 1974). The Bruker SHELXTL Version 5 system of programs was used for the refinement of the crystal structure.

TABLE 1. Miscellaneous information pertaining to the structure determination of parsonsite

a (Å)	6.842(4)	Crystal size (mm³)	0.08 × 0.03 × 0.005
b (Å)	10.383(6)	μ(mm⁻¹)	54.5
c (Å)	6.670(4)	D_{calc} (g/cm³)	6.317
α (°)	101.265(7)	Total ref.	5354
β (°)	98.174(7)	Unique ref.	2161
γ (°)	86.378(7)	R_{int} (%)	10.4
V (Å³)	459.8(7)	Unique $\lvert F_o\rvert \ge 4\sigma_F$	1187
Space group	$P\bar{1}$	Final *R** (%)	6.0
F(000)	732	*S*†	0.92

Unit-cell contents: $2\{Pb_2[(UO_2)(PO_4)_2]\}$

*$R = \Sigma(|F_o|-|F_c|)/\Sigma|F_o|$.
†$S = [\Sigma w(|F_o|-|F_c|)^2/(m-n)]^{1/2}$, for *m* observations and *n* parameters.

Reflection statistics indicated the space group $P\bar{1}$, which was verified by the successful solution of the structure by direct methods. Following refinement of the atomic positional parameters and isotropic displacement parameters for all atoms, the agreement factor (*R*) was 8.8 % for observed reflections. Conversion of the cation displacement parameters to anisotropic, together with refinement of the entire model, resulted in an *R* of 6.0% and a goodness-of-fit (*S*) of 0.92 for the 1187 unique observed ($|F_o| \ge 4\sigma_F$) reflections. A model including anisotropic displacement of the anions was tried, but it only lowered the final *R* by ~0.1%, and some of the displacement parameters became unrealistic. In the final cycle of refinement the average parameter shift/esd was 0.000. The minimum and maximum peaks in the final difference-Fourier maps were 3.77 and –3.19 e/Å³. The final atomic-positional parameters and anisotropic-displacement parameters are given in Tables 2 and 3, and selected interatomic-distances and angles are given in Table 4. Calculated and observed structure factors are provided in Table 5[1].

RESULTS

Cation coordination

The structure contains a single symmetrically unique U^{6+} cation. It is strongly bonded to two atoms of O in an approximately linear $(UO_2)^{2+}$ uranyl ion (Ur) with bond-lengths ~1.8 Å, as is almost invariably the case for U^{6+} in crystal struc-

TABLE 2. Atomic position parameters and equivalent isotropic-displacement parameters (U_{eq}, in Å² × 10⁻⁴) for the structure of parsonsite

	x	*y*	*z*	U_{eq}
U	0.6164(2)	0.8406(1)	0.1126(1)	231(3)
Pb1	0.3006(2)	0.5415(1)	0.2694(2)	300(3)
Pb2	0.0451(2)	0.7739(1)	0.7204(2)	336(3)
P1	0.534(1)	0.8187(6)	0.6302(9)	166(15)
P2	0.814(1)	0.5492(6)	0.278(1)	195(15)
O1	0.983(3)	0.636(2)	0.409(2)	211(39)
O2	0.335(3)	0.484(2)	0.597(3)	242(42)
O3	0.364(3)	0.785(2)	0.079(3)	340(48)
O4	0.665(3)	0.727(2)	0.762(3)	234(41)
O5	0.703(3)	0.625(2)	0.118(3)	281(44)
O6	0.336(3)	0.752(2)	0.536(3)	352(49)
O7	0.505(3)	0.060(2)	0.203(3)	229(40)
O8	0.855(3)	0.899(2)	0.141(3)	375(50)
O9	0.647(3)	0.854(2)	0.467(3)	309(46)
O10	0.915(3)	0.422(2)	0.168(3)	291(45)

TABLE 3. Anisotropic-displacement parameters (in Å² × 10⁻⁴) for the cations in the structure of parsonsite

	U_{11}	U_{22}	U_{33}	U_{12}	U_{13}	U_{23}
U	330(7)	214(6)	164(5)	33(4)	93(4)	41(4)
Pb1	298(7)	419(7)	200(6)	25(5)	86(5)	71(5)
Pb2	370(8)	314(7)	316(7)	18(5)	91(5)	16(5)
P1	263(41)	159(34)	78(31)	80(28)	38(27)	45(24)
P2	224(40)	192(35)	175(34)	29(28)	73(28)	27(26)

[1]For a copy of Table 5, document item AM-00-043, contact the Business Office of the Mineralogical Society of America (see inside front cover of recent issue) for price information. Deposit items may also be available on the American Mineralogist web site (http://www.minsocam.org or current web address).

tures (Burns et al. 1997c). The U^{6+} cation is coordinated by five additional anions arranged at the equatorial corners of a pentagonal bipyramid capped by O_{Ur} atoms. The <U-O_{Ur}> and <U-O_{eq}> (eq: equatorial) bond-lengths 1.78 and 2.39 Å, respectively, compare well with the average values obtained for [7]U in numerous well-refined structures, 1.79(4) and 2.37(9) Å, respectively (Burns et al. 1997c).

The structure contains two symmetrically distinct Pb^{2+} cations. Pb1 is coordinated by nine atoms of O, with Pb-O bond lengths ranging from 2.35 to 3.16 Å; <Pb1-O> = 2.75 Å. Three of the bond lengths are greater than 2.9 Å long, but are required to satisfy the bond-valence requirements of Pb1 (Fig. 2, Table 6). Pb2 is coordinated by six atoms of O, with a distinctly one-sided polyhedral geometry presumably owing to the presence of a lone pair of electrons on the cation. The Pb2-O bond lengths range from 2.28 to 3.15 Å; <Pb2-O> = 2.65 Å. Two Pb-O bond lengths greater than 2.9 Å are required to satisfy the bond-valence requirements of Pb2 (Table 6).

Each of the two symmetrically distinct P cations are tetrahedrally coordinated by O, with mean bond-lengths of 1.55 and 1.53 Å for the P1 and P2 sites, respectively.

Structural formula

All atomic sites are located on general positions in space group $P\bar{1}$. The bond-valence sums incident upon the O positions indicates that all correspond to O^{2-} (Table 6). The structural formula for the crystal studied is $Pb_2[(UO_2)(PO_4)_2]$. This formula differs from the formula given by Mandarino (1999) in the absence of H as H_2O. The final difference-Fourier maps were carefully inspected and did not reveal any additional atomic sites, suggesting that the crystal studied was anhydrous. Earlier studies of parsonsite indicate that the H_2O content is variable. Bignand (1955) synthesized anhydrous parsonsite and presented the same formula obtained in the current study. Frondel (1958) reported the water content in parsonsite is uncertain, and wrote the formula with one H_2O but indicated there may be 2 H_2O per formula unit. Mazzi et al. (1959) indicated the H_2O content of parsonsite varies from 0 to 2 H_2O per formula unit. More recently, Vochten et al. (1991) synthesized parsonsite with 0.5 H_2O per formula unit.

TABLE 4. Selected interatomic distances (Å) and angles (°) in the structure of parsonsite

U-O8	1.75(2)	Pb2-O1*e*	2.28(2)
U-O3	1.82(2)	Pb2-O10*d*	2.29(2)
U-O5	2.29(2)	Pb2-O6	2.46(2)
U-O9	2.32(2)	Pb2-O4*e*	2.74(2)
U-O7*a*	2.34(2)	Pb2-O3*f*	2.99(2)
U-O4*b*	2.46(2)	Pb2-O9*e*	3.15(2)
U-O7*c*	2.54(2)	<Pb2-O>	2.65
<U-O_{Ur}>	1.78		
<U-O_{eq}>	2.39	P1-O9	1.53(2)
<08-U3-03>	177.8(9)	P1-O7*d*	1.55(2)
		P1-O6	1.55(2)
Pb1-O2	2.35(2)	P1-O4	1.57(2)
Pb1-O6	2.54(2)	<P1-O>	1.55
Pb1-O2*d*	2.54(2)		
Pb1-O1*e*	2.55(2)	P2-O2*d*	1.50(2)
Pb1-O4*d*	2.76(2)	P2-O5	1.53(2)
Pb1-O5*c*	2.81(2)	P2-O10	1.55(2)
Pb1-O10*e*	2.92(2)	P2-O1	1.56(2)
Pb1-O3	3.12(2)	<P2-O>	1.53
Pb1-O10*c*	3.16(2)		
<Pbl-O>	2.75		
O9-P1-O7*d*	111.6(1.0)	O2d-P2-O5	107.0(1.0)
O9-P1-O6	112.9(1.1)	O2d-P2-O10	110.4(1.0)
O9-P1-O4	111.2(1.0)	O2d-P2-O1	113.7(1.0)
O7d-P1-O6	109.5(1.0)	O5-P2-O10	110.0(1.0)
O7d-P1-O4	101.5(9)	O5-P2-O1	108.9(1.0)
O6-P1-O4	109.5(1.0)	O10-P2-O1	106.8(1.0)
<O-P1-O>	109.4	<O-P2-O>	109.5

Notes: *a* = x, *y*+1, *z*; *b* = *x*, *y*, *z*–1; *c* = 1–*x*, 1–*y*, -*z*; d = 1–*x*, 1–*y*, 1–*z*; *e* = *x*–1, *y*, *z*; *f* = *x*, *y*, *z*+1. Ur = uranyl.

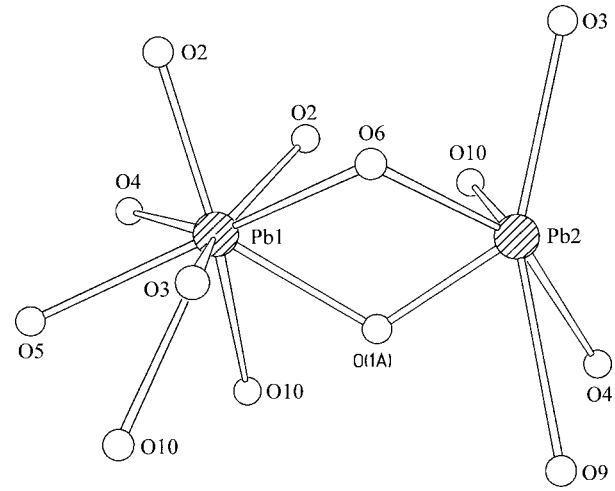

FIGURE 2. The Pb coordination polyhedra in parsonsite.

Structural connectivity

The structures of uranyl phosphate minerals previously known contain sheets based upon either the autunite or phosphuranylite anion-topologies (Fig. 1), and most uranyl mineral structures are based upon infinite sheets of polyhedra of higher bond-valence (Burns et al. 1996). Projection of the structure of parsonsite along [010] (Fig. 3) reveals that no sheets are present, thus parsonsite posses a new type of uranyl phosphate structure. The phosphate tetrahedra and uranyl pentagonal bipyramids are polymerized to form infinite chains parallel to [010], as shown in Figure 4.

Uranyl pentagonal bipyramids share an edge, resulting in dimers of composition $(UO_2)_2O_8$. Each uranyl polyhedron also shares an edge with a phosphate tetrahedron (P1), and the dimers of uranyl polyhedra are linked by phosphate-O_{eq} vertex sharing to form a chain. The P2 phosphate tetrahedra are linked to

TABLE 6. Bond-valence* sums (v.u.) for the structure of parsonsite

	U	Pb1	Pb2	P1	P2	Σ
O1		0.31	0.64		1.13	2.08
O2		0.53, 0.31			1.32	2.16
O3	1.55	0.07	0.09			1.71
O4	0.44	0.17	0.18	1.10		1.89
O5	0.62	0.15			1.22	1.99
O6		0.31	0.39	1.16		1.86
O7	0.56, 0.38			1.16		2.10
O8	1.78					1.78
O9	0.58		0.06	1.22		1.86
O10		0.11, 0.06	0.62		1.16	1.95
Σ	5.91	2.02	1.98	4.64	4.83	

* Bond-valence parameters for U^{6+} from Burns et al. (1997c), for Pb and P from Brese and O'Keeffe (1991).

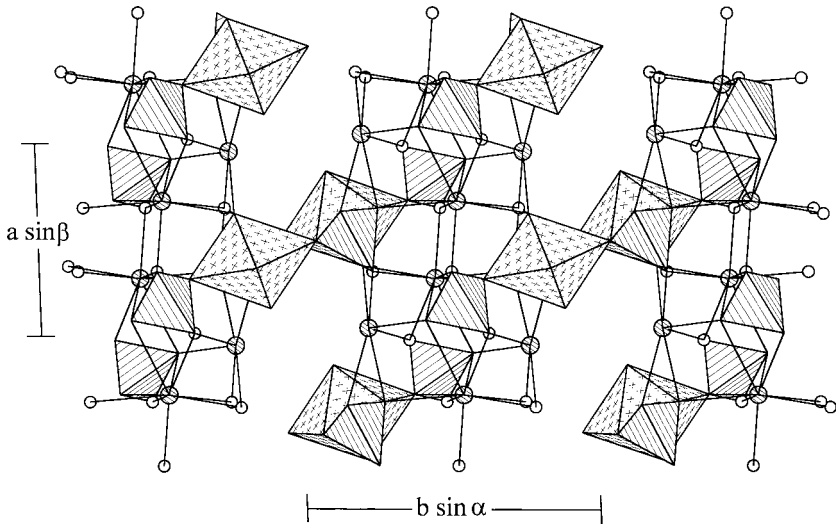

FIGURE 3. The structure of parsonsite projected along [001]. The uranyl polyhedra are shaded with crosses, the phosphate tetrahedra with parallel lines, O atoms are shown as open circles, and Pb atoms are shown as circles shaded with parallel lines.

the chain by vertex sharing only (Fig. 4). Layers of Pb polyhedra parallel to (010) (Fig. 3) link the uranyl phosphate chains.

DISCUSSION

In minerals the U^{6+} cation occurs as a $(UO_2)^{2+}$ uranyl ion that is coordinated by four to six O atoms or $(OH)^-$ groups located at the equatorial corners of bipyramids capped by the O_{Ur} atoms. The polyhedra involve a very asymmetric distribution of bond valences ($U\text{-}O_{Ur} \approx 1.7$ v.u., $U\text{-}O_{eq} \approx 0.5$ v.u.), usually resulting in sheets of polyhedra of higher bond-valence (Burns et al. 1996). Uranyl minerals with U as the only high-valence cation invariably contain sheets, as do uranyl vanadates, uranyl molybdates, and uranyl sulfates. Uranyl silicates contain sheets, except soddyite and weeksite, which involve frameworks of polyhedra of higher bond-valence. Uranyl carbonates are exceptional because they often contain isolated uranyl tricarbonate clusters, although rutherfordine and roubaultite contain uranyl carbonate sheets. The uranyl selenites demesmaekerite and derriksite contain chains of polyhedra, whereas guillemenite and haynesite both contain uranyl selenite sheets. Uranyl arsenates either contain autunite-type sheets, or chains, as in the structures of walpurgite and orthowalpurgite. Thus, the degree of polymerization depends upon the details of the high-valence cation polyhedra other than U.

Only a relatively small number of uranyl minerals posses structures based upon chains: moctezumite, derriksite, demesmaekerite, walpurgite, orthowalpurgite, and parsonsite (Fig. 5). With the exception of parsonsite, edge-sharing between polyhedra within the chains does not occur, nor do the uranyl polyhedra share polyhedral elements. The parsonsite chain is unusual because it involves edge-sharing between uranyl polyhedra, as well as between uranyl and phosphate polyhedra.

Burns et al. (1997c) examined polymerization in minerals and synthetic inorganic compounds that contain U. Phosphate tetrahedra share vertices with uranyl square bipyramids in the autunite-type sheet, and edges with uranyl hexagonal bipyramids in sheets that are based on the phosphuranylite-type anion topology. Ulrichite contains sheets of polyhedra that are based upon the uranophane anion-topology, with both CaO_7 and uranyl pentagonal bipyramids sharing edges with phosphate tetrahedra (Birch et al. 1988). However, several aspects of the ulrichite structure require further study. Thus, parsonsite is the first well-refined structure that involves edge-sharing between uranyl pentagonal bipyramids and phosphate tetrahedra. Assuming ideal polyhedral geometries, the equatorial edge-lengths of uranyl square, pentagonal and hexagonal bipyramids are 3.22, 2.79, and 2.47 Å, respectively (Burns et al. 1997c). An undistorted phosphate tetrahedron with a P-O bond-length of 1.53 Å (Shannon 1976) has an edge-length of 2.50 Å. Thus, edge-sharing between uranyl hexagonal bipyramids and phosphate tetrahedra requires essentially no polyhedral distortion, whereas the edge-lengths of uranyl square bipyramids and phosphate tetrahedra are different enough to make edge-sharing unlikely. Moderate distortion of the polyhedra is necessary for edge-sharing between uranyl pentagonal bipyramids and phosphate tetrahedra; presumably this explains why this mode of polymerization is less common than the sharing of edges between uranyl hexagonal bipyramids and phosphate tetrahedra.

ACKNOWLEDGMENTS

This research was funded by the Environmental Management Sciences Program of the United States Department of Energy (DE-FG07-97ER14820) and by the National Science Foundation (EAR98-04723).

REFERENCES CITED

Bignand, C. (1955) Sur les propiétés et les synthèses de quelques minéraux uranifères. Bulletin de la Société Francaise de Minéralogie et de la Cristallographie, 78, 1–26.

Birch, W.D., Mumme, W.G., and Segnit, E.R. (1988) Ulrichite: A new copper calcium uranium phosphate from Lake Boga, Victoria, Australia. Australian Mineralogist, 3, 125–131.

Brese, N.E. and O'Keeffe, M. (1991) Bond-valence parameters for solids. Acta Crystallographica, B47, 192–197.

Burns, P.C. (1998) CCD area detectors of X-rays applied to the analysis of mineral structures. Canadian Mineralogist, 36, 847–853.

———(1999) Cs boltwoodite obtained by ion exchange from single crystals: Implications for radionuclide release in a nuclear repository. Journal of Nuclear Materials, 265, 218–223.

Burns, P.C. and Finch, R.J. (1999) Wyartite: crystallographic evidence for the first

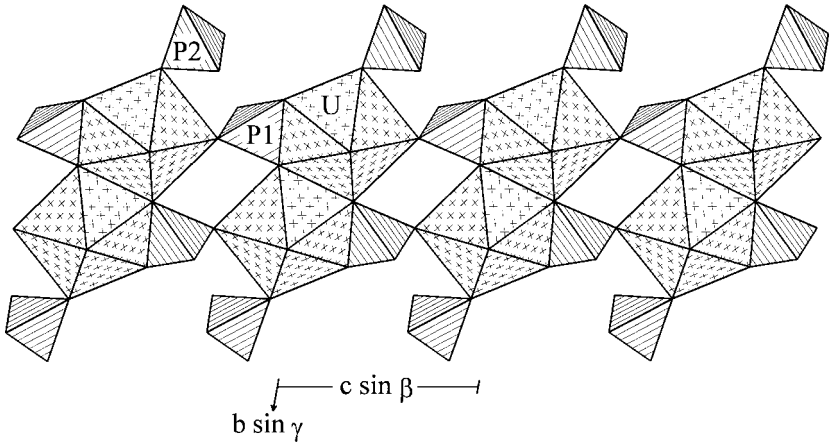

FIGURE 4. The uranyl phosphate chain in the structure of parsonite.

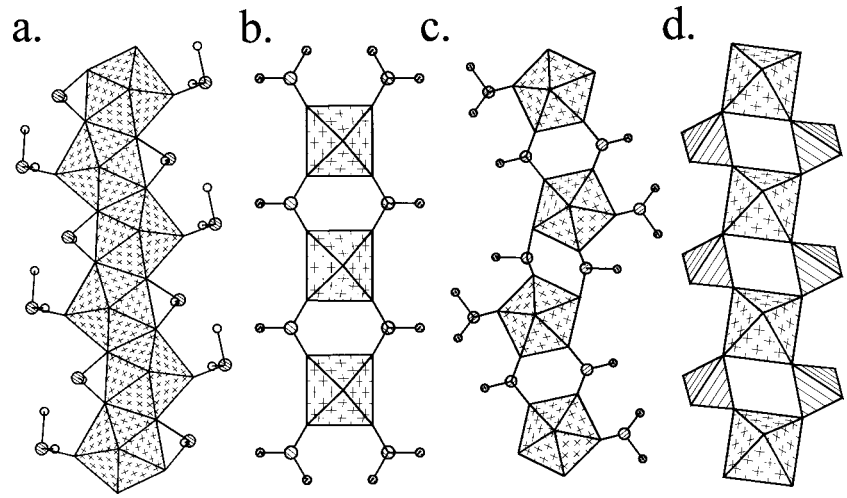

FIGURE 5. Chains of polyhedra that occur in uranyl minerals. (**a**) moctezumite, (**b**) derriksite, (**c**) demesmaekerite, (**d**) walpurgite and orthowalpurgite.

pentavalent-uranium mineral. American Mineralogist, 84, 1456–1460.
Burns, P.C., Miller, M.L., and Ewing, R.C. (1996) U^{6+} minerals and inorganic phases: a comparison and hierarchy of crystal structures. Canadian Mineralogist, 34, 845–880.
Burns, P.C., Ewing, R.C., and Miller, M.L. (1997a) Incorporation mechanisms of actinide elements into the structures of U^{6+} phases formed during the oxidation of spent nuclear fuel. Journal of Nuclear Materials, 245, 1–9.
Burns, P.C., Finch, R.J., Hawthorne, F.C., Miller, M.L., and Ewing, R.C. (1997b) The crystal structure of ianthinite, $[U_2^{4+}(UO_2)_4O_6(OH)_4(H_2O)_4](H_2O)_5$: A possible phase for Pu^{4+} incorporation during the oxidation of spent nuclear fuel. Journal of Nuclear Materials, 249, 199–206.
Burns, P.C., Ewing, R.C., and Hawthorne, F.C. (1997c) The crystal chemistry of hexavalent uranium: Polyhedral geometries, bond-valence parameters, and polyhedral polymerization. Canadian Mineralogist, 35, 1551–1570.
Finch, R.J. and Ewing, R.C. (1992) The corrosion of uraninite under oxidizing conditions. Journal of Nuclear Materials, 190, 133–156.
Finch, R.J., Hawthorne, F.C., and Ewing, R.C. (1998) Structural relations among schoepite, metaschoepite and "dehydrated schoepite". Canadian Mineralogist, 36, 831–845.
Finn, P.A., Hoh, J.C., Wolf, S.F., Slater, S.A., and Bates, J.K. (1996) The release of uranium, plutonium, cesium, strontium, technetium and iodine from spent fuel under unsaturated conditions. Radiochimica Acta, 74, 65–71.
Forsyth, R.S. and Werme, L.O. (1992) Spent fuel corrosion and dissolution. Journal of Nuclear Materials, 190, 3–19.
Frondel, C. (1958) Systematic Mineralogy of Uranium and Thorium. U.S. Geological Society Bulletin 1064, 400 p.
Ibers, J.A. and Hamilton, W.C., Eds. (1974) International Tables for X-ray Crystallography, IV. The Kynoch Press, Birmingham, U.K.
Johnson, L.H. and Werme, L.O. (1994) Materials characteristics and dissolution behavior of spent nuclear fuel. Material Research Society Bulletin, 24–27.
Mandarino, J.A. (1999) Fleischer's Glossary of Mineral Species 1999. The Mineralogical Record Inc., Tucson.
Mazzi, F., Garavelli, C.L., and Rinaldi, F. (1959) Dati ed osservazioni sulla cristallografia della parsonsite. Atti Society Toscana Science Natural A, 65, 135–146.
Murakami, T., Ohnuki, T., Isobe, H., and Sato, T. (1997) Mobility of uranium during weathering. American Mineralogist, 82, 888–899.
Pearcy, E.C., Prikryl, J.D., Murphy, W.M., and Leslie, B.W. (1994) Alteration of uraninite from the Nopal I deposit, Peña Blanca District, Chihuahua, Mexico, compared to °radation of spent nuclear fuel in the proposed U.S. high-level nuclear waste repository at Yucca Mountain, Nevada. Applied Geochemistry, 9, 713–732.
Shannon, R.D. (1976) Revised effective ionic radii and systematic studies of interatomic distances in halides and chalcogenides. Acta Crystallographica, A32, 751–767.
Smith, J.V. (1995) Synchrotron X-ray sources: Instrumental characteristics: New applications in microanalysis, tomography, absorption spectroscopy and diffraction. Analyst, 120, 1231–1245.
Sowder, A.G., Clark, S.B., and Fjeld, R.A. (1996) The effect of silica and phosphate on the transformation of schoepite to becquerelite and other uranyl phases. Radiochimica Acta, 74, 45–49.
Vochten, R., van Haverbeke, L., and van Springel, K. (1991) Transformation of chernikovite into parsonsite and study of its solubility product. Neues Jahrbuch für Mineralogie Monatshefte, 1991, 551–558.
Wronkiewicz, D.J., Bates, J.K., Wolf, S.F., and Buck, E.C. (1996) Ten-year results from unsaturated drip tests with UO_2 at 90°C: implications for the corrosion of spent nuclear fuel, Journal of Nuclear Materials, 238, 78–95.

MANUSCRIPT RECEIVED MARCH 23, 1999
MANUSCRIPT ACCEPTED DECEMBER 28, 1999
PAPER HANDLED BY GILBERTO ARTIOLI